

Stresses and velocities in orogenic wedges with power-law rheology and linearly varying longitudinal strain rate

JIYANG LIU and GIORGIO RANALLI

Department of Earth Sciences and Ottawa–Carleton Geoscience Centre, Carleton University,
Ottawa K1S 5B6, Canada
E-mail: granalli@ccs.carleton.ca

(Received 7 November 1996; accepted in revised form 30 March 1998)

Abstract—A two-dimensional analytical solution for stress, strain rate, and velocity is obtained for parallel-sided and wedge-shaped blocks with generalized viscous rheology (linearly viscous and power-law) deforming in plane strain. The main assumptions used in the derivation of the solution are that the material is incompressible, the longitudinal gradient in shear stress is much less than the vertical gradient of vertical normal stress, and the longitudinal strain rate varies linearly in the horizontal direction. Velocity boundary conditions are specified at the top of the block, and shear stress boundary conditions at the base of the block. In the one-dimensional case (where stress and strain rate do not vary in the longitudinal direction), the solution reduces to a well-known solution for the deformation of parallel-sided ice sheets [Nye, J. F. (1957) The distribution of stress and velocity in glaciers and ice sheets. *Proceedings of the Royal Society of London A-239*, 113–133]. The stress equilibrium for tapered wedges [Platt, J. P. (1986) Dynamics of orogenic wedges and the uplift of high-pressure metamorphic rocks. *Geological Society of America Bulletin* **97**, 1037–1053] is a special case of the present stress solution. Implementation of the solution requires the subdivision of the wedge into vertical segments, and yields the tectonic normal and shear stresses that must be applied to the rear of a block with specified rheology in order to maintain a given longitudinal strain rate. The solution makes it possible to model deformation patterns analytically with longitudinally varying strain rate (including coeval compression and extension) and with vertical components of velocity reflecting the effects of underplating. © 1998 Elsevier Science Ltd. All rights reserved

INTRODUCTION

Most models for orogenic wedges, notably the critical taper model, have focused on the dynamic equilibrium of foreland fold-and-thrust belts and accretionary prisms, i.e. supracrustal *thin-skinned* orogenic wedges which are usually less than 5–10 km thick at the rear (Elliott, 1976; Chapple, 1978; Davis *et al.*, 1983; Dahlen, 1984, 1990; Dahlen *et al.*, 1984; Dahlen and Suppe, 1988; Zhao *et al.*, 1986; Yin, 1989; Liu and Ranalli, 1992). These thin-skinned wedge models, however, do not account quantitatively for some features often observed in *thick-skinned* orogenic wedges involving basement rocks (Pavlis and Bruhn, 1983; Platt, 1986, 1987, 1993), namely: (a) coeval development of compressional structures at the thin-skinned foreland ‘front’ and extensional structures at the thick-skinned ‘rear’ towards the hinterland; (b) exhumation of high pressure–low temperature metamorphic rocks near the rear of the wedge; and (c) nonlinear rheology of materials (which is Coulomb frictional only in the upper parts, and most likely nonlinearly viscous in the bulk of the wedge; Platt, 1986, 1987, 1993; Liu and Ranalli, 1994; Ranalli, 1995; Liu, 1996).

Thus, the need exists for models incorporating the nonlinear bulk rheology of thick-skinned wedges. Analytical solutions for nonlinear (power-law) viscous rheology exist in glaciology (Nye, 1951, 1957, 1969; Budd, 1970; Shoemaker and Morland, 1984). One of these is the classic ice sheet solution obtained by Nye

(1957) for incompressible plane strain flow. Because of the similarities between the movement of glaciers and ice sheets and that of nappes and thrust sheets (Elliott, 1976), this solution has been applied to the analysis of shortening and elongating thrust sheets (Wojtal, 1992a,b). Since it does not specify *a priori* the stress exponent n for the material, it is sufficiently general to accommodate a wide range of deformation modes which might be applicable to thick orogenic wedges: linear Newtonian flow ($n = 1$), power-law creep ($n = 2 \sim 4$), and perfect plasticity ($n \rightarrow \infty$). However, Nye’s solution is applicable only to parallel-sided sheets with uniform shortening or extending flows, since it is based on the assumptions that the stress tensor depends on depth only and that the vertical velocity component does not vary with longitudinal position. The constancy of longitudinal strain rate makes this solution unsuitable to the modelling of thick-skinned orogenic wedges where the deformation pattern varies not only in the vertical but also in the longitudinal direction.

In this paper we present a two-dimensional plane strain analytical solution for stresses and velocities in blocks and wedges with nonlinear rheology. This solution removes some of the conditions limiting Nye’s (1957) solution, and is therefore applicable to cases where the strain rate varies in the longitudinal direction. It reduces to Nye’s solution in the one-dimensional case. The focus of the argument is on the procedure for obtaining a closed-form solution, and

not on computational details. However, the results of four model tests are given, to show the potential applicability of the solution to thick-skinned orogenic wedges.

GOVERNING EQUATIONS

The geometry of the model, coordinate system, and sign convention for stresses are given in Fig. 1. The equilibrium condition for two-dimensional incompressible power-law flow is (*cf.* e.g. Ranalli, 1995)

$$\begin{aligned} \frac{\partial \sigma_{xx}}{\partial x} + \frac{\partial \sigma_{xy}}{\partial y} + \rho g_x &= 0 \\ \frac{\partial \sigma_{xy}}{\partial x} + \frac{\partial \sigma_{yy}}{\partial y} + \rho g_y &= 0 \end{aligned} \quad (1)$$

where σ_{ij} is the stress tensor, ρ the density, and g_i the acceleration of gravity. The rheological equations are

$$\begin{aligned} \dot{\epsilon}_{xx} &= \lambda \sigma'_{xx} \\ \dot{\epsilon}_{yy} &= \lambda \sigma'_{yy} \\ \dot{\epsilon}_{xy} &= \lambda \sigma'_{xy} \end{aligned} \quad (2)$$

where σ'_{ij} is the stress deviator, $\dot{\epsilon}_{ij}$ is the strain rate tensor, and λ is a stress-dependent parameter having dimensions of reciprocal viscosity. The strain rate tensor is related to velocity components u, v in the x, y direction as

$$\begin{aligned} \dot{\epsilon}_{xx} &= \frac{\partial u}{\partial x} \\ \dot{\epsilon}_{yy} &= \frac{\partial v}{\partial y} = -\frac{\partial u}{\partial x} \\ \dot{\epsilon}_{xy} &= \frac{1}{2} \left(\frac{\partial u}{\partial y} + \frac{\partial v}{\partial x} \right) \end{aligned} \quad (3)$$

and the stress deviator is given by

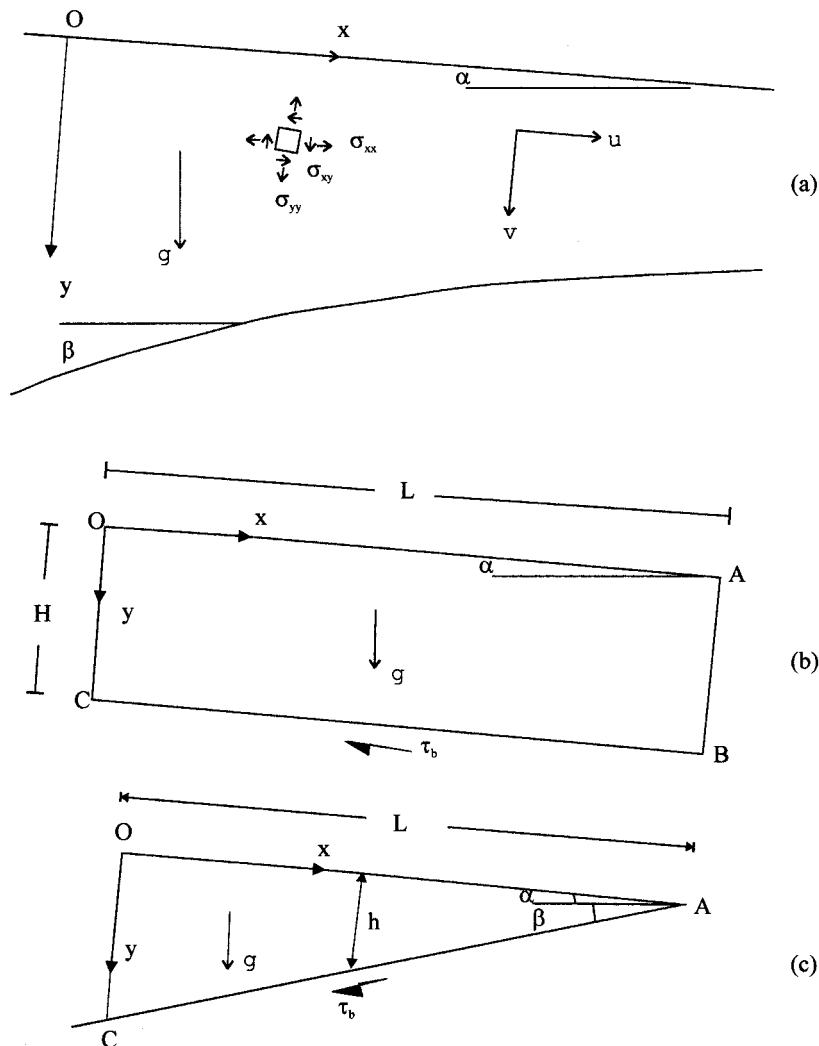


Fig. 1. (a) Simplified two-dimensional orogenic wedge model: α is the surface slope, β the basal slope, u, v the velocity components, and g the acceleration of gravity; positive stress components are shown. (b) Parallel-sided block and (c) wedge-shaped block. τ_b is basal shear stress, h is local wedge thickness.

$$\begin{aligned}\sigma'_{xx} &= \frac{1}{2}(\sigma_{xx} - \sigma_{yy}) \\ \sigma'_{yy} &= \frac{1}{2}(\sigma_{yy} - \sigma_{xx}) = -\sigma'_{xx} \\ \sigma'_{xy} &= \sigma_{xy}\end{aligned}\quad (4)$$

The explicit form of the parameter λ in equation (2) for power-law creep is (cf. e.g. Ranalli, 1995)

$$\lambda = A_0 \exp\left(-\frac{Q + PV}{RT}\right) \left(\frac{1}{2}\sigma'_{ij}\sigma'_{ij}\right)^{(n-1)/2} \quad (5)$$

where T is absolute temperature, P pressure, R the universal gas constant, and Q , V , A_0 and n are material parameters [Q and V are the creep activation energy and activation volume, respectively; the term PV is negligible when $P \ll k$ (bulk modulus) as is the case in the crust]. The parameter λ becomes independent of the state of stress if the rheology of the material is Newtonian ($n = 1$).

A TWO-DIMENSIONAL LINEAR LONGITUDINAL STRAIN RATE SOLUTION

Basic assumptions

Four assumptions are adopted in the derivation of the present solution:

1. The longitudinal strain rate $\dot{\epsilon}_{xx}$ varies linearly in the longitudinal direction at any point within the wedge

$$\frac{\partial^2 \dot{\epsilon}_{xx}}{\partial x^2} = 0 \quad (6)$$

2. The gradient of shear stress in the x -direction is negligible compared with the gradient of vertical normal stress in the y -direction

$$\left|\frac{\partial \sigma_{xy}}{\partial x}\right| \ll \left|\frac{\partial \sigma_{yy}}{\partial y}\right| \quad (7)$$

3. The wedge material is incompressible and in plane strain

$$\frac{\partial u}{\partial x} + \frac{\partial v}{\partial y} = 0 \quad (8)$$

4. The density varies with depth only

$$\frac{\partial \rho}{\partial x} = 0. \quad (9)$$

It should be noted that the terms 'horizontal' and 'vertical' are used in this paper in the sense of 'x-direction' and 'y-direction'. Since the surface slope angle α is

usually small ($\alpha \leq 6^\circ$, cf. Boyer and Elliot, 1982; Suppe, 1985), this has no major consequences.

The first assumption [equation (6)] greatly simplifies the problem while still allowing the simulation of syn-convergence extension, which is a first-order feature of many orogenic wedges (Pavlis and Bruhn, 1983; Platt, 1986, 1987, 1993). The introduction of this assumption implies that the problem becomes that of finding force boundary conditions at the rear of the wedge resulting in a linearly varying longitudinal strain rate and realistic fault patterns. Consequently, the validity of the assumption is tested *a posteriori* from the success of the solution to model realistic tectonic forces and deformation. The second assumption [equation (7)] is generally held to be correct to the first order and has been adopted in numerous studies (Elliott, 1976; Boyer and Elliott, 1982; Davis *et al.*, 1983; Dahlen, 1984; Suppe, 1985; Platt, 1986; Liu and Ranalli, 1992, 1994; Yin, 1988, 1989, 1993). The third assumption [equation (8)] should be a good approximation whenever the material is well lithified (cf. Dahlen and Barr, 1989 for details); however, it is not valid when there is large volume reduction due to loss of fluids. The fourth assumption [equation (9)] is simply a first approximation to the usual density variations in the upper crust of the Earth.

Derivation of solution

A general stress solution to equation (1) under the second assumption [equation (7)] is

$$\begin{aligned}\sigma_{xx} &= -\bar{\rho}g_y y + F(y) - xG'(y) \\ \sigma_{yy} &= -\bar{\rho}g_y y \\ \sigma_{xy} &= -\bar{\rho}g_x y + G(y)\end{aligned}\quad (10)$$

where $\bar{\rho}$ is the depth-averaged density and $F(y)$, $G(y)$ are two arbitrary functions of depth. Physically, $F(y)$ and $G(y)$ are the non-gravitational (i.e. tectonic) normal and shear stress components applied on the rear of the block (Fig. 2).

Using the stress solution [equation (10)] in the expressions for strain rate [equation (2)] and taking into account equation (4), the strain rate components are

$$\begin{aligned}\dot{\epsilon}_{xx} &= \lambda \sigma'_{xx} = \frac{\lambda}{2} [F(y) - xG'(y)] \\ \dot{\epsilon}_{yy} &= \lambda \sigma'_{yy} = -\frac{\lambda}{2} [F(y) - xG'(y)] \\ \dot{\epsilon}_{xy} &= \lambda \sigma'_{xy} = \lambda [G(y) - \bar{\rho}g_x y]\end{aligned}\quad (11a)$$

where the parameter λ as defined in equation (5), can be expressed in terms of the stress solution as

$$\lambda = B_0 \left\{ \frac{1}{4} [F(y) - xG'(y)]^2 + [G(y) - \bar{\rho}g_x y]^2 \right\}^{(n-1)/2} \quad (11b)$$

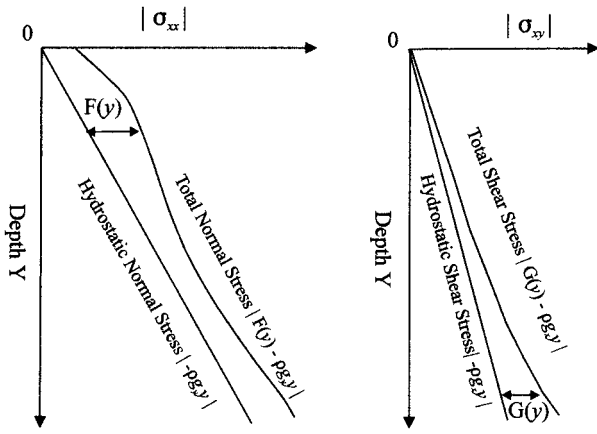


Fig. 2. State of stress along the wedge rear boundary ($x = 0$). The stress axis refers to magnitude. According to the adopted sign convention, $F(y) < 0$ when compressive; $G(y) < 0$ when shearing downwards.

where $B_0 = A_0 \exp\left(-\frac{Q+PV}{RT}\right)$ is a function of temperature, pressure and material parameters [see equation (5)].

The general expressions for the velocity components are obtained by integrating the first two of equation (3) with respect to x and y , respectively,

$$u(x, y) = \frac{1}{2} \int_0^x \lambda(\zeta, y) [F(y) - xG'(\zeta)] d\zeta + H(y)$$

$$v(x, y) = -\frac{1}{2} \int_0^y \lambda(x, \tau) [F(\tau) - xG'(\tau)] d\tau + I(x) \quad (12)$$

where $I(x)$ and $H(y)$ are two integration functions. Physically, $H(y)$ is the vertical distribution of the longitudinal velocity component at the rear of the block, since $H(y) = u(x = 0, y)$; and $I(x)$ is the longitudinal distribution of vertical velocity component at the surface, since $I(x) = v(x, y = 0)$.

Combination of the four assumptions [equations (6)–(9)] and appropriate boundary conditions allow all the integration functions appearing in equations (10)–(12) to be expressed as functions of $F(y)$ and seven arbitrary constants ($a_1, a_2, a_3, b_1, b_2, b_3, b_4$). The details of the derivation are given in the Appendix. The final expressions for stress, strain rate and velocity are

$$\sigma_{xx} = -\bar{\rho}g_y y + \left(1 + \frac{a_1 + b_1 y}{a_2 + b_2 y} x\right) F(y)$$

$$\sigma_{yy} = -\bar{\rho}g_x y$$

$$\sigma_{xy} = -\int_0^y \left[\rho g_x + \frac{a_1 + b_1 \tau}{a_2 + b_2 \tau} F(\tau) \right] d\tau \quad (13a)$$

$$\dot{\epsilon}_{xx} = -(a_1 + b_1 y)x - (a_2 + b_2 y)$$

$$\dot{\epsilon}_{yy} = -\dot{\epsilon}_{xx}$$

$$\dot{\epsilon}_{xy} = \frac{2(a_2 + b_2 y)}{F(y)} \int_0^y \left[\rho g_x + \frac{a_1 + b_1 \tau}{a_2 + b_2 \tau} F(\tau) \right] d\tau \quad (13b)$$

$$u = -\frac{x^2}{2} (a_1 + b_1 y) - x(a_2 + b_2 y) - \frac{b_1}{6} y^3 - \frac{a_1}{2} y^2 - b_3 y$$

$$- a_3 + 4 \int_0^y \left\{ \frac{a_2 + b_2 \zeta}{F(\zeta)} \int_0^\zeta \left[\rho g_x + \frac{a_1 + b_1 \tau}{a_2 + b_2 \tau} F(\tau) \right] d\tau \right\} d\zeta$$

$$v = \frac{b_1}{6} x^3 + \frac{b_2}{2} x^2 + x \left(\frac{b_1}{2} y^2 + a_1 y + b_3 \right)$$

$$+ \frac{b_2}{2} y^2 + a_2 y + b_4 \quad (13c)$$

The parameter λ in equation (2) can be written in terms of $F(y)$ and arbitrary constants as $\lambda = -2(a_2 + b_2 y)/F(y)$, which, when combined with equations (5) and (11b), links the function $F(y)$ with the rheology of the block through the following expression

$$-\frac{2(a_2 + b_2 y)}{F(y)B_0} = \left\{ \left[\frac{F(y)}{2} \left(1 + \frac{a_1 + b_1 y}{a_2 + b_2 y} x \right) \right]^2 \right.$$

$$\left. + \left[\int_0^y \left(\rho g_x + \frac{a_1 + b_1 \tau}{a_2 + b_2 \tau} F(\tau) \right) d\tau \right]^2 \right\}^{(n-1)/2} \quad (13d)$$

Equations (13a–d) constitute a complete general solution for a two-dimensional block with power-law rheology and linear longitudinal strain rate. The general solution is equally applicable to rectangular blocks and to triangular wedges (refer to Fig. 1).

Discussion of the solution

Several points about equation (13) should be noted:

1. There are two kinds of unknowns which are involved in equation (13), and need to be determined from boundary conditions: the function $F(y)$, and seven constants of integration. The function $F(y)$ is related to some of the integration constants [cf. equation (13d)]. According to their kinematic implications, these seven constants can be classified into two groups: those related to longitudinal strain rate (a_1, a_2, b_1 and b_2), and those related to rigid-body motion corresponding to velocity and rotation at the origin (a_3, b_3 and b_4).
2. The state of stress at the rear of the block ($x = 0$), represented by the functions $F(y)$ and $G(y)$, is related to rheology and strain rate [cf. equation (13d) and (A6) in the Appendix]. The solution therefore requires $F(y)$ to be computed for a given rheology and prescribed strain rate. Physically, therefore, $F(y)$ is the tectonic normal stress required at the rear of a block with given material rheology and temperature distribution to maintain a given longitudinal strain rate. Another possible way of applying

equation (13d) is to compute the strain rate for a given rheology and independently specified $F(y)$. However, this approach leads to severe difficulties, since it is not feasible to ensure the compatibility of the specified $F(y)$ with the given rheology and temperature distribution.

3. The assumption of linear longitudinal strain rate [equation (6)] requires the parameter λ to be a function of y only [see equation (A5) in the Appendix]. This results in the left side of equation (13d) being a function of y only while the right side is a function of both x and y . This apparent paradox is the direct consequence of the linearity assumption for the longitudinal strain rate. To demonstrate the impact of this assumption on the relation between strain rate and deviatoric stress [i.e. equation (2)], we have derived other closed-form solutions based on different assumptions for the longitudinal strain rate. For example, assuming that the longitudinal strain rate at any depth y is a cubic polynomial function of position x (i.e. $\partial^4 \dot{\epsilon}_{xx} / \partial x^4 = 0$), we obtain another set of solutions for stress, strain rate and velocity. Both sides of the corresponding equation (13d) for this new set of solutions are functions of x and y . Although it is much more complicated, this new set of solutions can be reduced to the simpler solution reported in this paper if we degrade the assumption on the longitudinal strain rate from a cubic polynomial function of x into a linear function of x . Obviously, the complexity of the solution increases with the complexity of the assumed x -dependence of longitudinal strain rate. On the other hand, the significant benefit of the linearity assumption is the relative simplicity of the derived analytical solution.

Numerically, this difficulty is solved by dividing the wedge into vertical segments of width Δx and applying equation (13) to each segment, within which the longitudinal variation of deviatoric normal stress is negligible. Physically, the interdependence of tectonic stress and longitudinal strain rate is a consequence of the rheological properties of the wedge. Mathematically, the determination of $F(y)$ from equation (13d) is a *two-point boundary value problem*, which is solved here by the so-called shooting method (for detailed discussion see Press *et al.*, 1992).

For a typical wedge segment with a longitudinal width less than 10 km, the longitudinal variation of the computed function $F(y)$ is less than 5% (Liu, 1996). A smooth variation of the solution for stress, strain rate and velocity from one segment to the next supports its validity. Continuity for adjacent Δx is achieved by linear interpolation.

Two sets of boundary conditions are specified for each segment: three points on the top boundary with assigned velocity and one point on the basement with assigned basal shear stress. The state of stress along

the basement, together with the smoothness of the solution in the whole wedge, is another test of the validity of the present approach. The required basal shear stress τ_b should be smooth, either constant or increasing from the front to the rear, and of reasonable magnitude (0–100 MPa).

COMPARISON BETWEEN TWO-DIMENSIONAL AND ONE-DIMENSIONAL SOLUTIONS

The linear longitudinal strain rate solution given by equation (13) is a two-dimensional extension of the classic one-dimensional solution for glacier flow (Nye, 1957). Table 1 compares the two solutions in detail, and shows that the present solution reduces to Nye's for $a_1 = b_1 = b_2 = b_3 = 0$, which is equivalent to the assumption $\partial v / \partial x = 0$ used in Nye's analysis. In the one-dimensional solution, both the second stress invariant and the shear stress are assumed to be independent of longitudinal position. In the two-dimensional solution, the less restrictive assumption that the longitudinal gradient in shear stress is negligible compared with the vertical gradient in vertical normal stress results in a horizontal normal deviatoric stress which is a linear function of longitudinal position. This allows a more complex velocity field to be accommodated.

COMPARISON WITH EQUILIBRIUM CONDITION FOR TAPERED WEDGES

In this section, we compare the present solution with Platt's dynamic stability criterion for orogenic wedges (Platt, 1986), and show that this criterion is a particular case of the present stress solution.

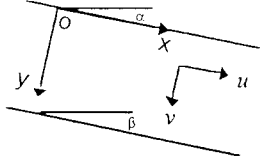
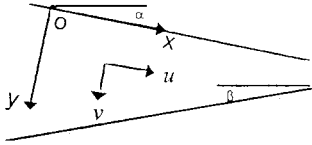
Assuming an unspecified viscous rheology, Platt (1986) derived a stability criterion for two-dimensional plane strain thick orogenic wedges, which relates the basal shear stress (τ_b) to the topographic slope (α), the depth-averaged longitudinal deviatoric stress (τ_{xx}) and its longitudinal gradient acting in a tapered wedge (*cf.* Fig. 3)

$$\tau_b = \rho g h \alpha - 2\tau_{xx}\theta - 2\frac{\partial \tau_{xx}}{\partial x} h \quad (14)$$

where $\theta (= \alpha + \beta)$ is the taper of the wedge, h the local thickness of the wedge, ρ density, and g gravity.

It should be pointed out that an additional implicit assumption is needed in Platt's model in order to derive equation (14). This is that the longitudinal deviatoric stress τ_{xx} be equal to zero on the upper surface of the wedge. This assumption is used when integration with respect to y is performed on the stress equilibrium equation in the x -direction [see equations (11) and (12) in Platt, 1986]. This additional condition means that the near-surface part of the

Table 1. Comparison between one-dimensional solution (Nye, 1957) and the present two-dimensional solution.

1-D solution* (Nye, 1957)	present 2-D solution
model geometry and rheology	
 <p>The basement is parallel to the top surface ($\alpha = \beta$); power-law rheology is postulated as a function of depth y only</p>	 <p>The basement and top surface may dip in opposite directions; power-law rheology varies both longitudinally and vertically</p>
model assumptions	
<p>(1) incompressible plane strain flow; (2) stress tensor is function of depth only; (3) density is function of depth only; (4) $\partial v / \partial x = 0$</p>	<p>(1) incompressible plane strain flow; (2) $\partial \sigma_{xy} / \partial x \ll \partial \sigma_{xy} / \partial y$; (3) density is function of depth only; (4) $\partial^2 \dot{\epsilon}_{xx} / \partial x^2 = 0$</p>
stress solution	
$\sigma_{xx} = -\bar{\rho} g_y y + F(y)$ $\sigma_{yy} = -\bar{\rho} g_y y$ $\sigma_{xy} = -\bar{\rho} g_x x y$ $-\frac{2a_2}{F(y)} = A \tau_E'^{n-1}$	$\sigma_{xx} = -\bar{\rho} g_y y + \left[1 + \frac{a_1 + b_1 y}{a_2 + b_2 y} x \right] F(y)$ $\sigma_{yy} = -\bar{\rho} g_y y$ $\sigma_{xy} = -\bar{\rho} g_x x y - \int_0^y \frac{a_1 + b_1 \tau}{a_2 + b_2 \tau} F(\tau) d\tau$ $-\frac{2(a_2 + b_2 y)}{F(y)} = A \tau_E'^{n-1}$
strain rate solution	
$\dot{\epsilon}_{xx} = -a_2$ $\dot{\epsilon}_{yy} = a_2$ $\dot{\epsilon}_{xy} = \frac{2a_2 \bar{\rho} g_x y}{F(y)}$	$\dot{\epsilon}_{xx} = -(a_1 + b_1 y)x - (a_2 + b_2 y)$ $\dot{\epsilon}_{yy} = (a_1 + b_1 y)x + (a_2 + b_2 y)$ $\dot{\epsilon}_{xy} = \frac{2(a_2 + b_2 y)}{F(y)} \left[\frac{\bar{\rho} g_x y}{a_2 + b_2 y} + \int_0^y \frac{a_1 + b_1 \tau}{a_2 + b_2 \tau} F(\tau) d\tau \right]$
velocity solution	
$u = -a_2 x + 4a_2 g_x \int_0^y \frac{\bar{\rho} \tau}{F(\tau)} d\tau - a_1$ $v = a_2 y + b_1$	$u = -\frac{a_1}{2} (x^2 + y^2) - a_2 x - a_1 - \frac{b_1}{2} y \left(x^2 + \frac{y^2}{3} \right) - b_2 x y$ $- b_3 y + 4 \int_0^y \left\{ \frac{a_2 + b_2 \zeta}{F(\zeta)} \left[\frac{\bar{\rho} g_x \zeta}{a_2 + b_2 \zeta} + \int_0^\zeta \frac{a_1 + b_1 \tau}{a_2 + b_2 \tau} F(\tau) d\tau \right] \right\} d\zeta$ $v = a_1 x y + a_2 y + \frac{b_1}{2} x \left(\frac{x^2}{3} + y^2 \right) + \frac{b_2}{2} (x^2 + y^2) + b_3 x + b_4$

*Minor modifications to Nye's original expressions have been made to facilitate comparison.

wedge is always under a nearly lithostatic state of stress.

To recast the present stress solution [equation (13a)] in a format that is directly comparable with Platt's model, the longitudinal deviatoric stress (σ'_{xx}) and the depth-averaged longitudinal deviatoric stress (τ_{xx}) are computed from equation (13a)

$$\sigma'_{xx} = \frac{F(y) - xG'(y)}{2}$$

$$\frac{\partial \tau_{xx}}{\partial x} = \frac{\partial}{\partial x} \left[\frac{1}{h} \int_0^h \sigma'_{xx} dy \right] = -\frac{1}{2h} \int_0^h G'(y) dy = -\frac{G(h)}{2h} \quad (15)$$

where h is the thickness of the wedge at the point

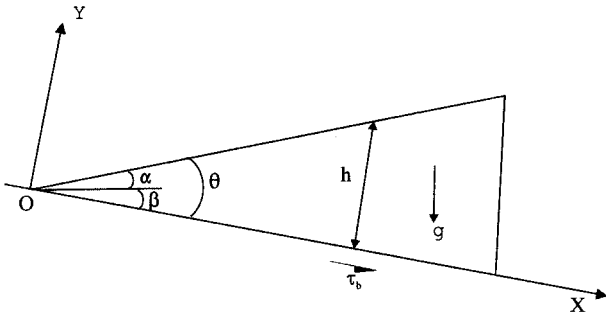


Fig. 3. Platt's accretionary wedge model and its coordinates (Platt, 1986): α and β are the top and basal slopes, respectively; $\theta (= \alpha + \beta)$ is the taper of the wedge, h thickness, and τ_b basal shear stress.

under consideration. The basal shear stress τ_b is related to the state of stress within the wedge as (*cf.* e.g. Ranalli, 1995)

$$\begin{aligned} \tau_b &= \frac{1}{2}(\sigma_{yy} - \sigma_{xx})_{y=h} \sin 2\theta - (\sigma_{xy})_{y=h} \cos 2\theta \\ &\approx \bar{\rho}gh\alpha - \theta[F(y) - xG'(y)]_{y=h} - G(h) \end{aligned} \quad (16)$$

Combining equations (15) and (16) leads to

$$\tau_b = \bar{\rho}gh\alpha - 2\theta(\sigma'_{xx})_{y=h} + 2h \frac{\partial \tau_{xx}}{\partial x} \quad (17)$$

where small-angle approximations for α and θ are used.

Comparison of equations (14) and (17) shows two differences: (1) the signs of the third term on the right side are different; and (2) the stress component in the second term on the right side of equation (17) is the longitudinal deviatoric stress on the basement (i.e. $y = h$) while the corresponding term in equation (14) is the depth-averaged longitudinal deviatoric stress. The sign difference is a trivial consequence of the

difference in coordinate systems (compare Figs 1c & 3). The second difference is caused by the aforementioned assumption about the stress state along the wedge upper surface.

Therefore, Platt's (1986) stability criterion is compatible with—indeed, it is a particular case of—the stress solution derived in this paper, subject to the assumption that the longitudinal deviatoric stress does not vary significantly along any depth profile. This condition most likely holds in thin-skinned wedges but may not be satisfied in thick-skinned wedges, where deformation patterns may vary significantly in the vertical direction.

EXAMPLES

Four examples of the two-dimensional solution are discussed in this section. The first two are rectangular blocks with Newtonian and power-law rheologies; the remaining two are wedges with Newtonian and power-law rheologies. The parameter values used in the computations are listed in Table 2. All cases are parameterized in the following way:

(a) The velocity boundary conditions along the top surface are of the general form

$$\begin{aligned} u_{\text{top}} &= u_0 + u_1 x + u_2 x^2 \\ v_{\text{top}} &= v_0 + v_1 x \end{aligned} \quad (18a)$$

where u_0 , u_1 , u_2 , v_0 and v_1 are constants. Assuming that displacements of the top and the base of the block are related, this boundary condition can represent indirectly basal underplating and basal erosion.

Table 2. Model parameters for rectangular and wedge-shaped blocks

Parameter	Rectangular block ($L = 250$ km, $\alpha = \beta = 3^\circ$, $\rho = 2800$ kg m $^{-3}$)		Wedge block ($L = 200$ km, $\alpha = 3^\circ$, $\beta = 6^\circ$, $\rho = 2700$ kg m $^{-3}$)	
	A	B	C	D
u_0 ($\times 10^{-10}$ m s $^{-1}$)	31.71†	31.71	0	0
u_1 ($\times 10^{-15}$ s $^{-1}$)	-1	-1	-1	1
u_2 ($\times 10^{-20}$ m $^{-1}$ s $^{-1}$)	0	0	-2.25	-1
v_0 ($\times 10^{-10}$ m s $^{-1}$)	-0.4	-0.4	-1.5855	-1.5855
v_1 ($\times 10^{-15}$ s $^{-1}$)	0	0	0.7927	0.7927
τ_0 (MPa)	-57.44	-57.44	-80	-80
τ_1 (MPa km $^{-1}$)	0	0	0.4	0.4
T_0 (K)	‡	750	‡	750
T_1 (K km $^{-1}$)	‡	2.5	‡	0
A_0^* ($\times 10^{-23}$ Pa $^{-1}$ s $^{-1}$)	5	‡	5	‡
A_1^* ($\times 10^{-23}$ Pa $^{-1}$ s $^{-1}$ km $^{-1}$)	0	‡	0	‡
power-law rheology	‡	anorthosite§	‡	anorthosite§

*Cases A, B, C, and D refer to Figs 4–7, respectively.

A: Newtonian, constant η (10^{22} Pa s), constant $\dot{\epsilon}_{xx}$ and constant v on surface, constant τ_b .

B: Power-law, depth-dependent T , constant $\dot{\epsilon}_{xx}$ and constant v on surface, constant τ_b .

C: Newtonian, constant η (10^{22} Pa s), variable $\dot{\epsilon}_{xx}$ and variable v on surface, variable τ_b .

D: Power-law, constant T , variable $\dot{\epsilon}_{xx}$ and variable v on surface, variable τ_b .

† 100 mm a $^{-1} \approx 31.71 \times 10^{-10}$ m s $^{-1}$.

‡ not applicable (constant Newtonian viscosity or computed power-law viscosity).

§ rheological parameters: $A_0 = 2.06 \times 10^{-23}$ Pa $^{-3.2}$ s $^{-1}$, $n = 3.2$, $Q = 238$ kJ mol $^{-1}$.

- (b) The basal shear stress along the basement is a linear function of position

$$\tau_b = \tau_0 + \tau_1 x \tag{18b}$$

where τ_0 and τ_1 are constants.

- (c) The temperature within the block is either constant or varies linearly with depth

$$T = T_0 + T_1 y \tag{18c}$$

where T_0 and T_1 are constants.

- (d) The rheology of the block can be nonlinear (stress exponent $n > 1$) or linear ($n = 1$). In case of linear rheology, Newtonian viscosity is assumed to be of the form

$$\eta = \frac{1}{2(A_0^* + A_1^* y)} \tag{18d}$$

where A_0^* and A_1^* are constants. This allows the viscosity to be either constant or decreasing with depth.

The first example (Fig. 4) serves as a reference case for a rectangular block with constant Newtonian viscosity ($\eta = 10^{22}$ Pa s) and constant basal shear stress. The top velocity boundary condition is such that the u component varies linearly with x (resulting in a constant longitudinal strain rate of $\dot{\epsilon}_{xx} = -10^{-15}$ s⁻¹ on the upper surface of the block) and the v component is

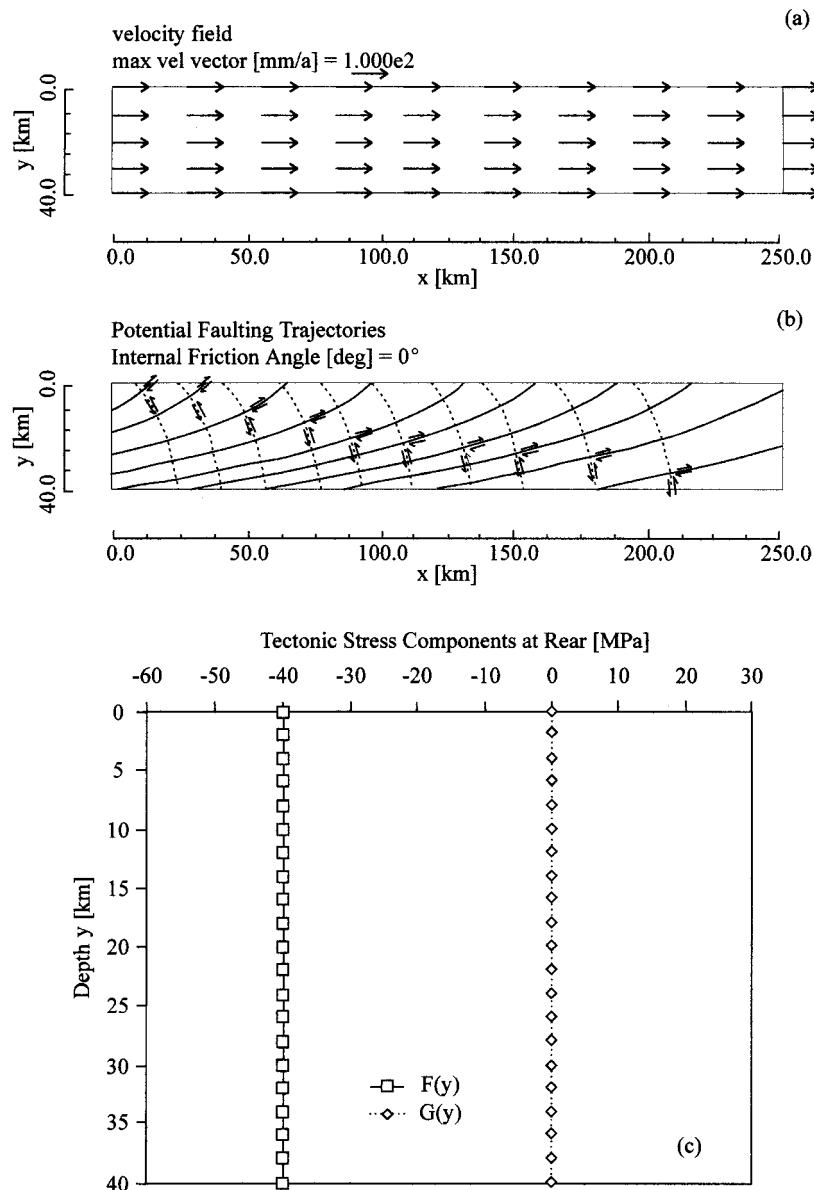


Fig. 4. Stress and deformation within a rectangular block with Newtonian rheology (case A of Table 2). (a) Velocity field; (b) maximum shear stress trajectories and type of potential faults; (c) tectonic (non-gravitational) normal and shear stresses along the rear of the block.

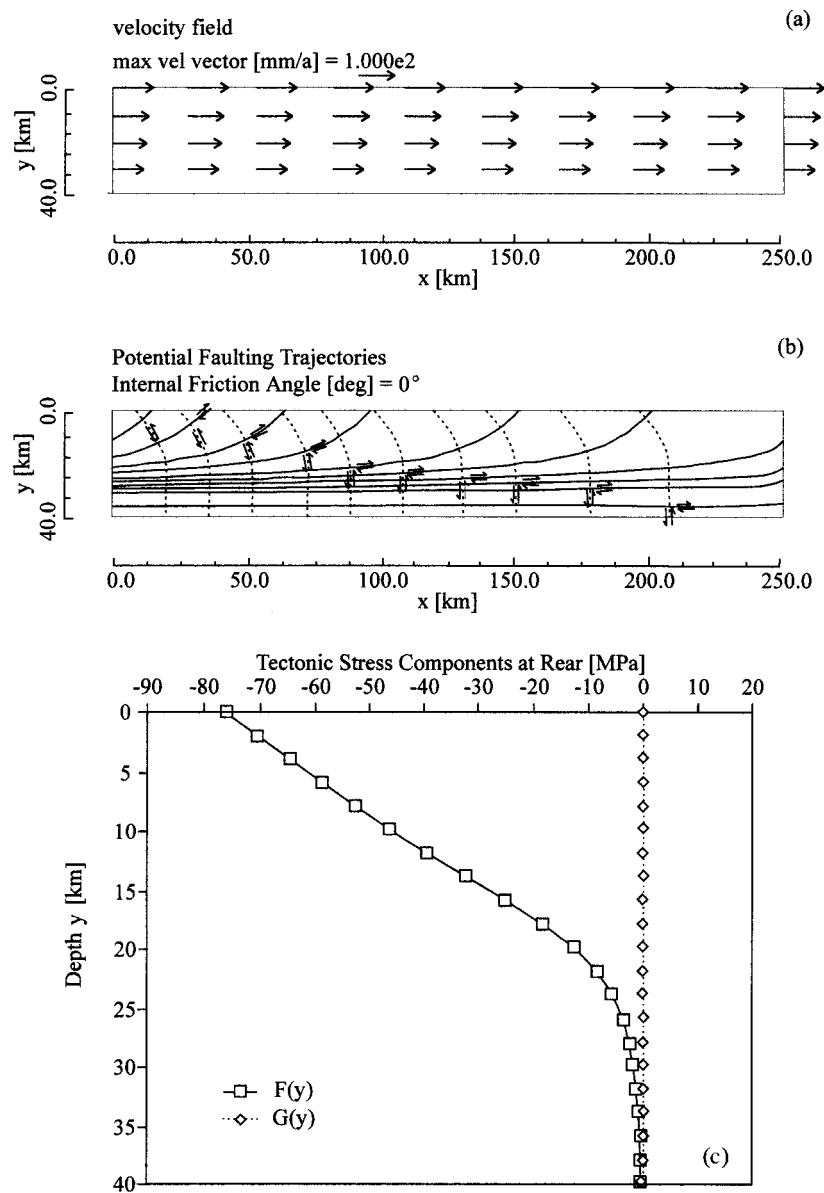


Fig. 5. Stress and deformation within a rectangular block with power-law rheology (case B of Table 2). (a), (b) & (c) as in Fig. 4.

constant. This velocity boundary condition is compatible with Nye's one-dimensional solution (Nye, 1957). Consequently, results for this case yield simply a two-dimensional representation of Nye's one-dimensional solution in the case of Newtonian viscosity. Figure 4 shows (a) the velocity field within the block; (b) the maximum shear stress trajectories, which coincide with potential faulting surfaces in a frictionless (plastic) material; (c) the depth distribution of the 'non-gravitational' normal and shear stress components [i.e. the functions $F(y)$ and $G(y)$] along the rear vertical edge of the block (note that a tectonic compression is required to maintain the deformation regime).

The second example (Fig. 5) considers a rectangular block of nonlinear rheology with the power-law creep parameters of anorthosite (*cf.* Ranalli, 1995) and the same velocity and basal shear stress boundary con-

ditions as in the previous case. The temperature increases from 750 K on the top to 850 K at the bottom of the block (the relatively large temperature at the top is necessary to yield realistic strain rates, given the rheology of the material). Even this low temperature gradient increases considerably the ductility of the material: predominant laminar flow is found near the base of the block. $F(y)$ decreases in magnitude non linearly from about 76 MPa at the top to about 0 MPa at the bottom of the block.

The third example (Fig. 6) consists of a wedge with constant Newtonian viscosity ($\eta = 10^{22}$ Pa s) and a longitudinal component of the top velocity boundary condition resulting in a longitudinal strain rate $\dot{\epsilon}_{xx}$ varying from -10^{-15} s $^{-1}$ at the rear to -10^{-14} s $^{-1}$ at the front of the wedge. The velocity boundary conditions result in a dominant movement pattern of

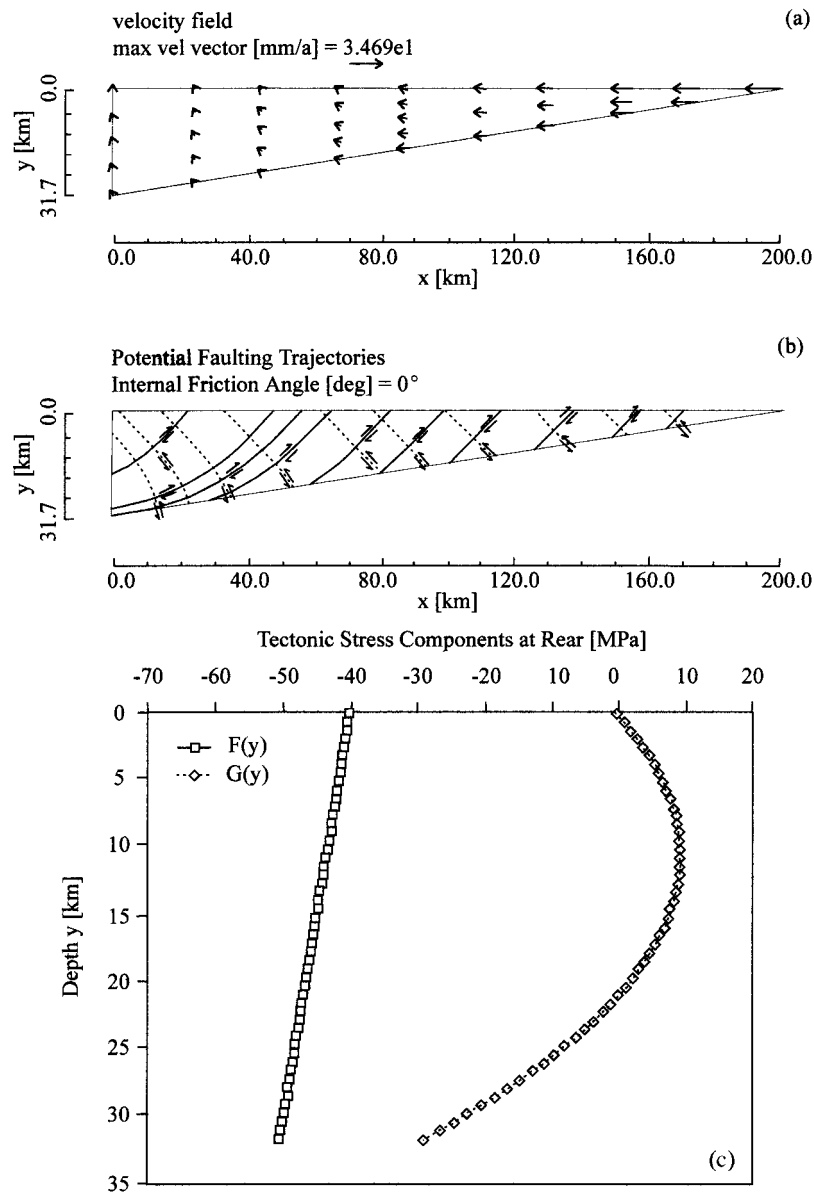


Fig. 6. Stress and deformation within a wedge-shaped block with Newtonian rheology (case C of Table 2). (a), (b) & (c) as in Fig. 4.

wedge material which is longitudinal at the front, and mainly vertical towards the rear (for instance, as resulting from increasing underplating). The maximum shear stress trajectories show thrust deformation throughout the wedge. $F(y)$ increases in magnitude from 40 MPa at the top to 50 MPa at the bottom of the wedge; $G(y)$ varies roughly in a parabolic way with depth.

The fourth example (Fig. 7) considers a wedge with the power-law rheology of anorthosite and with a constant temperature of 750 K. The longitudinal strain rate $\dot{\epsilon}_{xx}$ on the top surface of the wedge varies linearly from -10^{-15} s^{-1} at the rear to $-3 \times 10^{-15} \text{ s}^{-1}$ at the front. There is some underplating near the rear of the wedge as in the previous case (note the different velocity scale in the figures). The maximum shear stress trajectories show coeval development of an extensional

regime (potential normal faulting) at the rear and a compressional regime (thrusting) at the front of the wedge. The non-gravitational normal stress at the rear of the wedge necessary to maintain this deformation regime is tensional: $F(y)$ decreases nonlinearly from about 80 MPa on the top to about 10 MPa at the bottom of the wedge. The depth distribution of $G(y)$ is similar to the previous case.

DISCUSSION AND CONCLUSIONS

We have presented an analytical linear longitudinal strain rate solution for blocks and wedges with non-linear rheology ($n \geq 1$), which is a two-dimensional extension of the classic one-dimensional solution derived by Nye (1957) for ice sheets. This solution allows

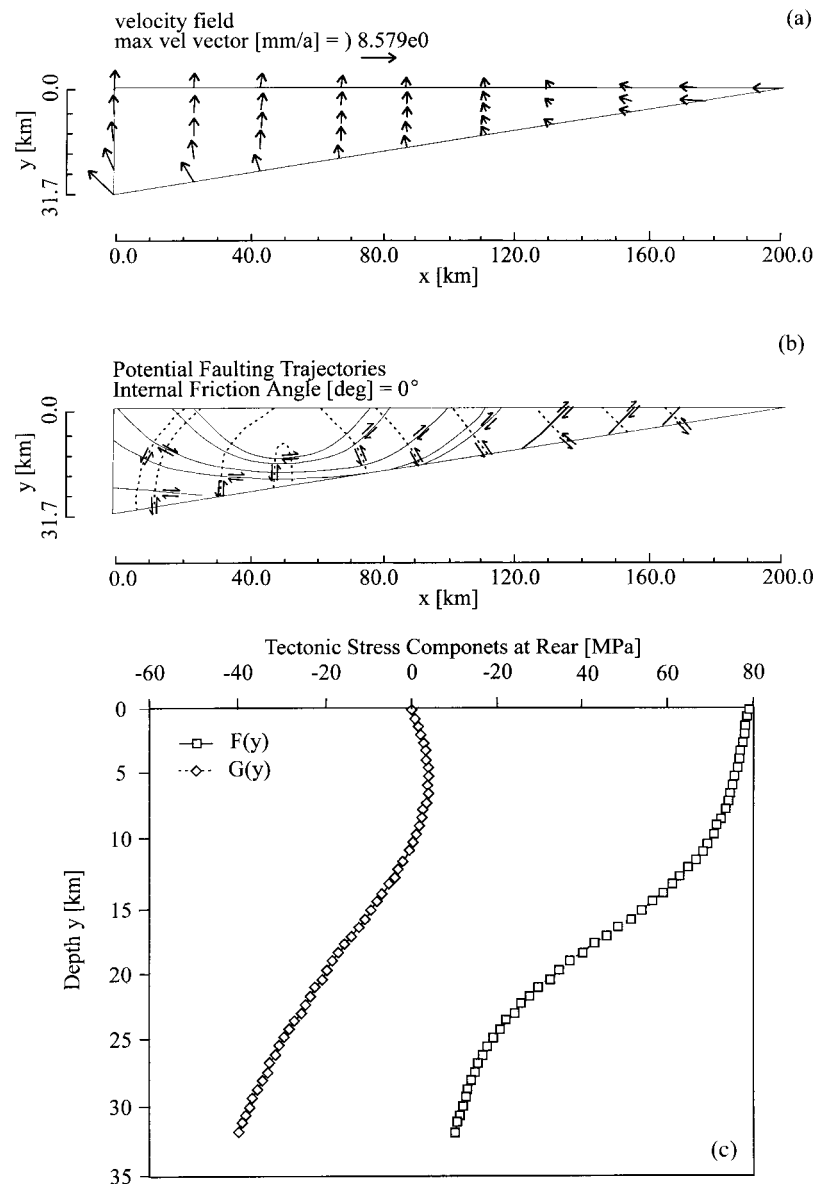


Fig. 7. Stress and deformation within a wedge-shaped block with power-law rheology (case D of Table 2). (a), (b) & (c) As in Fig. 4.

the modelling of stresses and deformation in two-dimensional orogenic wedges with deformation styles varying in the longitudinal direction.

The basic kinematic assumption is that the longitudinal strain rate, at any depth, is a linear function of the distance from the rear of the block. Together with wedge segmentation, this assumption allows the simulation of varying deformation patterns, including coeval compression and extension, in different parts of the wedge. The specification of velocity boundary condition on the surface of the block significantly simplifies the implementation of the solution. A more complicated algorithm would be needed to specify the velocity boundary conditions on the basement rather than on the top surface. However, kinematic conditions on the top of an incompressible block may be taken as a first approximation to conditions at the bot-

tom, for instance, with an upward component of velocity simulating underplating.

In the solution, the nongravitational stresses $F(y)$ and $G(y)$ along the rear vertical boundary of the block are derived quantities, i.e. they are the tectonic stresses necessary to maintain the specified linear longitudinal strain rate for a given rheology under specified top (velocity) and bottom (shear stress) boundary conditions (this approach is the same as the one taken in the one-dimensional solution; Nye, 1957). Alternatively, they could be assigned *a priori* as part of the boundary conditions, but this is not possible in the framework of the present solution. It remains to be discussed, in any particular case, whether the required normal and shear tectonic stresses are realistic. In the four simple examples considered, their magnitudes are of the right order, being comprised between ± 80 MPa.

Their distribution varies with depth, but is generally rather simple. If *a priori* knowledge of $F(y)$ and $G(y)$ is assumed, it is still possible, within the framework of the present solution, to modify iteratively the boundary conditions until the required tectonic stress distribution is satisfactorily approximated.

The linear strain rate solution can also be applied to investigate the evolution of wedges with varying taper, by solving iteratively for different surface slopes. In this context, it is also relevant to the problem of the exhumation of high pressure–low temperature metamorphic rocks near the rear of an unstable orogenic wedge (Rubie, 1984; Platt and Lister, 1985; Platt, 1993). Combined with a given erosion rate at the top surface of the wedge, the velocity expression of the solution [equation (13c)] provides an estimation of the exhumation rate and, therefore, of the time variation of the pressure–temperature conditions of rocks throughout the wedge. Assuming that the surface erosion rate is the same as the rate at which material is uplifted at the basement of the wedge, the exhumation rate at the rear of the wedge of the fourth example would be about 6 mm per y (Fig. 7). This is, of course, an upper boundary since it assumes that no additional topography is generated.

Naturally, the rheology of orogenic wedges is more complicated than power-law throughout. As the temperature decreases approaching the surface, plastic–brittle deformation takes over. In principle, this change can be accommodated by the present solution, by letting the stress exponent increase (pure plasticity requires $n \rightarrow \infty$), and ensuring that the deformation patterns in the power-law and plastic domains are compatible (Liu, 1996). Despite the limitations imposed by its analytical character, the solution presented in this paper has the advantage of *generality*, and provides an additional approach to the study of the tectonic evolution of orogenic wedges.

Acknowledgements—This paper represents part of the doctoral dissertation by one of the authors (J. L.). The work was supported by NSERC (Natural Sciences and Engineering Research Council of Canada) grants to G. R. and by a Carleton University Scholarship to J. L. We thank P.-Y. Robin and K. Rohr for constructive reviews.

REFERENCES

- Boyer, S. and Elliott, D. (1982) Thrust systems. *American Association of Petroleum Geologists Bulletin* **66**, 1196–1230.
- Budd, W. F. (1970) The longitudinal stress and strain-rate gradients in ice masses. *Journal of Glaciology* **9**, 19–47.
- Chapple, W. M. (1978) Mechanics of thin-skinned fold-and-thrust belts. *Geological Society of America Bulletin* **89**, 1189–1198.
- Dahlen, F. A. (1984) Noncohesive critical Coulomb wedges: An exact solution. *Journal of Geophysical Research* **89**, 10,125–10,133.
- Dahlen, F. A. (1990) Critical taper model of fold-and-thrust belts and accretionary wedges. *Annual Review of Earth and Planetary Sciences* **18**, 55–99.
- Dahlen, F. A. and Barr, T. D. (1989) Brittle frictional mountain building I, Deformation and mechanical energy budget. *Journal of Geophysical Research* **94**, 3906–3922.
- Dahlen, F. A. and Suppe, J. (1988) Mechanics, growth, and erosion of mountain belts. In *Processes in Continental Lithospheric Deformation*, eds S. P. Clark Jr, B. C. Burchfiel and J. Suppe. pp. 161–208. Geological Society of America Special Paper, **218**.
- Dahlen, F. A., Suppe, J. and Davis, D. M. (1984) Mechanics of fold-and-thrust belts and accretionary wedges: cohesive Coulomb theory. *Journal of Geophysical Research* **89**, 10,087–10,101.
- Davis, D. M., Suppe, J. and Dahlen, F. A. (1983) Mechanics of fold-and-thrust belts and accretionary wedges. *Journal of Geophysical Research* **89**, 1153–1172.
- Elliott, D. (1976) The motion of thrust sheets. *Journal of Geophysical Research* **81**, 949–963.
- Liu, J. Y. (1996) Stress and Deformation in Orogenic Wedges with Power-Law Rheology. Ph.D. thesis. Carleton University, Ottawa.
- Liu, J. Y. and Ranalli, G. (1992) Stress in an overthrust sheet and propagation of thrusting: An Airy stress function solution. *Tectonics* **11**, 549–559.
- Liu, J. Y. and Ranalli, G. (1994) A two-dimensional power-law rheology model for subduction-accretionary orogenic complexes (Abstract). *EOS* **75**, 598.
- Nye, J. F. (1951) The flow of glaciers and ice-sheets as a problem in plasticity. *Proceedings Royal Society of London A* **207**, 554–572.
- Nye, J. F. (1957) The distribution of stress and velocity in glaciers and ice sheets. *Proceedings Royal Society of London AA* **239**, 113–133.
- Nye, J. F. (1969) The effect of longitudinal stress on the shear stress at the base of an ice sheet. *Journal of Glaciology* **8**, 207–213.
- Pavlis, T. L. and Bruhn, R. L. (1983) Deep-seated flow as a mechanism for the uplift of broad forearc ridges and its role in the exposure of high P/T metamorphic terranes. *Tectonics* **2**, 473–497.
- Platt, J. P. (1986) Dynamics of orogenic wedges and the uplift of high-pressure metamorphic rocks. *Geological Society of America Bulletin* **97**, 1037–1053.
- Platt, J. P. (1987) The uplift of high-pressure–low-temperature metamorphic rocks. *Philosophical Transactions Royal Society of London, A* **321**, 87–103.
- Platt, J. P. (1993) Exhumation of high-pressure rocks. *Terra Nova* **5**, 119–133.
- Platt, J. P. and Lister, G. S. (1985) Structural history of high-pressure metamorphic rocks in the Vanoise massif, French Alps, and their relation to Alpine tectonic events. *Journal of Structural Geology* **7**, 19–36.
- Press, W. H., Teukolsky, S. A., Vetterling, W. T. and Flannery, B. P. (1992) *Numerical recipes*. 2nd edn. Cambridge University Press, Cambridge.
- Ranalli, G. (1995) *Rheology of the Earth*, 2nd edn. Chapman & Hall, London.
- Rubie, D. C. (1984) A thermal-tectonic model for high-pressure metamorphism and deformation in the Sesia zone, western Alps. *Journal of Geology* **92**, 21–36.
- Shoemaker, E. M. and Morland, L. W. (1984) A glacier flow model incorporating longitudinal deviatoric stress. *Journal of Glaciology* **30**, 334–339.
- Spiegel, M. R. (1971) *Schaum's Outline of Theory and Problems of Advanced Mathematics for Engineers and Scientists*. McGraw-Hill, New York.
- Suppe, J. (1985) *Principles of Structural Geology*. Prentice-Hall, Englewood Cliffs.
- Wojtal, S. (1992a) One-dimensional models for plane and non-plane power-law flow in shortening and elongating thrust zones. In *Thrust tectonics*, ed. K. R. McClay, pp. 41–52. Chapman & Hall, London.
- Wojtal, S. (1992b) Shortening and elongation of thrust zones within the Appalachian foreland fold-thrust belt. In *Structural Geology of Fold and Thrust Belts*, eds S. Mitra and G. W. Fisher, pp. 93–103. Johns Hopkins University Press, Baltimore.
- Yin, A. (1988) Geometry, kinematics, and a mechanical analysis of a strip of the Lewis allochthon from Peril Peak to Bison Mountain, Glacier National Park, Montana. Ph.D. thesis. University of Southern California, Los Angeles.
- Yin, A. (1989) Origin of regional, rooted low-angle normal faults: a mechanical model and its implications. *Tectonics* **8**, 469–482.
- Yin, A. (1993) Mechanics of wedge-shaped fault blocks I, an elastic solution for compressional wedges. *Journal of Geophysical Research* **98**, 14,245–14,256.

Zhao, W. L., Davis, D. M., Dahlen, F. A. and Suppe, J. (1986)
 Origin of convex accretionary wedges: evidence from Barbados.
Journal of Geophysical Research **91**, 10,246–10,258.

APPENDIX

In this Appendix, we derive the general solution given in the text [equation (13)].

Differentiating the first of equation (11a) twice with respect to x and combining it with equation (6) leads to

$$\frac{F(y) - xG'(y)}{2} \frac{\partial^2 \lambda}{\partial x^2} - G'(y) \frac{\partial \lambda}{\partial x} = 0 \tag{A1}$$

which is a second-order partial differential equation which can be transformed into a first-order equation and then solved by standard procedures (*cf.* Spiegel, 1971).

A general solution to equation (A1) is

$$\lambda = \frac{k(y)}{F(y) - xG'(y)} + f_0(y) \tag{A2}$$

where $k(y)$ and $f_0(y)$ are two integration functions.

Combination of equations (A2) and (11a) with the equation of compatibility for two-dimensional plane strain (*cf.* e.g. Ranalli, 1995) gives

$$\begin{aligned} & \frac{\partial^2 \dot{\epsilon}_{xx}}{\partial y^2} + \frac{\partial^2 \dot{\epsilon}_{yy}}{\partial x^2} - 2 \frac{\partial^2 \dot{\epsilon}_{xy}}{\partial x \partial y} = \frac{1}{2} k''(y) \\ & + \frac{1}{2} \frac{d^2}{dy^2} [f_0(y)F(y)] - \frac{x}{2} \frac{d^2}{dy^2} [f_0(y)G'(y)] \\ & + 2 \frac{G'(y)k(y)[G'(y) - \rho g_x] + [G(y) - \bar{\rho} g_{xy}] \frac{d}{dy} [k(y)G'(y)]}{[F(y) - xG'(y)]^2} \\ & - 4 \frac{G'(y)k(y)[F(y) - xG''(y)][G(y) - \bar{\rho} g_{xy}]}{[F(y) - xG'(y)]^3} = 0 \end{aligned} \tag{A3}$$

where the double prime denotes the second derivative with respect to y .

Equation (A3) contains several terms that are functions of x of different orders. In order that equation (A3) be satisfied at all points, one of following three conditions must apply

$$(a) \begin{cases} k(y) = 0 \\ f_0(y)G'(y) = 2(a_1 + b_1y) \\ f_0(y)F(y) = -2(a_2 + b_2y) \end{cases} \tag{A4a}$$

$$(b) \begin{cases} G'(y) = 0 \\ \frac{1}{2} k''(y) + \frac{1}{2} \frac{d^2}{dy^2} [f_0(y)F(y)] = 0 \end{cases} \tag{A4b}$$

$$(c) \begin{cases} G(y) = \bar{\rho} g_{xy} \\ f_0(y)G'(y) = 2(a_1 + b_1y) \\ \frac{1}{2} k''(y) + \frac{1}{2} \frac{d^2}{dy^2} [f_0(y)F(y)] = 0 \end{cases} \tag{A4c}$$

where a_1, a_2, b_1 and b_2 are arbitrary constants.

The second condition [equation (A4b)] represents a stress field corresponding to flow of a material compressed between two parallel plates (Nye, 1957), and is not applicable to an orogenic wedge with variable longitudinal deformation pattern. The third condition [equation (A4c)] is not applicable either, because it is a stress field with zero shear stress everywhere in the wedge, which is not able to produce any shear deformation. Therefore, only the first case [equation (A4a)] is relevant.

Equation (A4a) gives

$$\begin{aligned} \lambda &= f_0(y) = -\frac{2(a_2 + b_2y)}{F(y)} \\ G'(y) &= -\frac{a_1 + b_1y}{a_2 + b_2y} F(y) \end{aligned} \tag{A5}$$

Integrating the second of equations (A5) with respect to y gives

$$G(y) = -\int_0^y \frac{a_1 + b_1\tau}{a_2 + b_2\tau} F(\tau) d\tau \tag{A6}$$

where the traction-free boundary condition on the surface of the wedge [i.e. $G(0) = 0$] has been used to determine the integration constant. Equation (A6) implies that the normal and shear stress components of non-gravitational stress along the rear boundary of the wedge are not independent of each other.

The velocity integration functions $I(x)$ and $H(y)$ in equation (12) can be determined by combining equations (A5), (A6) and (11a) with (2). After some algebra, we have

$$\begin{aligned} I(x) &= \frac{b_1}{6} x^3 + \frac{b_2}{2} x^2 + b_4 \\ H(y) &= 4 \int_0^y \left\{ \frac{a_2 + b_2\zeta}{F(\zeta)} \int_0^\zeta \left[\rho g_x + \frac{a_1 + b_1\tau}{a_2 + b_2\tau} F(\tau) \right] d\tau \right\} d\zeta \\ &\quad - \frac{b}{6} y^3 - \frac{a_1}{2} y^2 - b_3 y - a_3 \end{aligned} \tag{A7}$$

where a_3, b_3 and b_4 are arbitrary constants.

Thus, all the integration functions for stress, strain rate, and velocity have been expressed as functions of seven arbitrary constants and the function $F(y)$, the horizontal nongravitational stress on the rear of the block.